NUMERICAL SIMULATION AND EXPERIMENTAL RESEARCH ON COMPACTION DEVICE OF SEEDBED LEVELING MACHINE
/
苗床整平机镇压夯实装置数值模拟与试验研究

Bo-jun SHAN [1,2)], Gang CHE[*1,2)], Lin WAN [*1,2)], Nai-chen ZHAO [1)], Qiang ZHANG [1)]
[1)]College of Engineering, Heilongjiang Bayi Agricultural University, Daqing/P.R.China
[2)]Key Laboratory of Intelligent Agricultural Machinery Equipment in Heilongjiang Province, Daqing / P.R.China
Tel：+86-459-13836961617；E-mail: chegang180@126.com;
DOI: https://doi.org/10.35633/inmateh-74-04

Keywords: *impeller type, fertilizer discharger, EDEM, variable, experiment*

ABSTRACT
Currently, the compaction operations in rice seedling greenhouses are mostly performed manually or with simple machinery, resulting in significant discrepancies between the operational effects and requirements. Moreover, simple compaction machinery towed by small tractors cannot meet the dimensional requirements of rice seedling greenhouses. To address the issues of limited types of rice seedling compaction machinery and inability to meet the technical requirements for seedbed compaction quality, an eccentric compaction mechanism suitable for use in rice seedling greenhouses has been designed to reduce manual labor and improve soil firmness and evenness of seedbeds. Based on eccentric vibration theory, the motion equation of the leveling machine was established, and numerical simulations of the eccentric compaction mechanism were conducted using the RecurDyn-EDEM coupling method. Results indicate that the eccentric compaction mechanism effectively resolves the inability of traditional compaction devices to meet soil firmness requirements. Using a seedbed leveling machine independently developed by Heilongjiang Bayi Agricultural University, parameter optimization experiments were conducted using a second-order orthogonal rotational combination simulation method. The optimized parameter combination was: forward speed of 0.708 m/s, eccentric shaft rotation speed of 63.23 rad/s, and counterweight box mass of 50.99 kg, resulting in soil firmness of 3156.554 kPa and evenness of 0.02573 m. The experimental results were within 5% relative error of the simulation optimization results, indicating that the seedbed soil firmness and evenness meet agronomic requirements and have practical application value.

摘要
目前水稻育秧大棚中的镇压夯实作业多为人力或简易机械完成，其作业效果与要求相差较大，且简易镇压机械由小型拖拉机牵引作业，无法适应水稻育秧大棚中的尺寸要求。针对水稻育秧镇压机械种类少，压实质量无法满足育秧苗床的技术要求问题，设计一种适用于水稻育秧大棚内的偏心镇压夯实机构，用于减少人力提高苗床土壤坚实度以及平整度。基于偏心激振理论，建立整平机运动方程，通过运用 Recurdyn-EDEM 耦合的方法对偏心镇压夯实机构进行数值模拟。结果表明：采用偏心镇压夯实机构有效解决传统镇压装置无法满足土壤坚实度要求。采用黑龙江八一农垦大学自主研发苗床整平机，应用二次正交旋转组合仿真试验方法进行参数优化试验，优化参数组合：机车前进速度为 0.708 m/s，偏心轴转速为 63.23 rad/s，配重箱质量为 50.99 kg 时，土壤坚实度为 3156.554 kpa，平整度为 0.02573 m。试验结果与仿真优化结果相对误差在 5%之内，苗床土壤坚实度以及平整度达到农艺要求具有实际应用价值。

INTRODUCTION
In modern agricultural production, soil compaction is a crucial step in improving crop yield and quality. However, current agricultural compaction machinery is limited in variety and often too large to meet the dimensional requirements of greenhouse environments. Within greenhouses, compaction operations are mostly carried out manually by dragging heavy objects, resulting in significant discrepancies between operational effects and requirements, making large-scale application challenging.

[1]*Bo-jun Shan, master degree; Gang Che, Prof. Ph.D.; Lin Wan, Prof. Ph.D.; Nai-chen Zhao, Ph.D.; Qiang Zhang master degree;*

Wang Jia L. et al. designed a variable pressure seedling belt compactor that can detect the compaction force during field operations of seeders through pressure sensors and digital displays, and adjust the force via a hydraulic system. They also analyzed the impact of compaction force on actual seed depth and plant spacing, thereby optimizing the appropriate range of compaction force *(Jia L., Jiang Y., Sun J., et al., 2021).* Luo Hongqi et al. researched a combination compactor capable of simultaneously compacting ridge sides and seeding bands *(Luo H., Meng Y., Li X., 2019)*. The compaction wheel's soil contact area is circular, resulting in an arched ridge shape post-compaction, which is beneficial for maintaining ridge form. Ren Luquan et al., addressing soil adhesion issues during compaction roller operations, designed a bionic compaction roller *(Zhang Y., Huang H., Ren L., 2013)*. This design incorporates a flexible rubber sleeve around the traditional roller body, with protruding ribs on the inner surface of the flexible outer sleeve creating a gap between the rubber sleeve and the roller body. This allows for deformation and vibration of the flexible outer sleeve during operation, thereby reducing soil adhesion to the roller. Foreign research on compaction implements is more extensive, with over 200 types of compactors in the United States alone. For example, contour-following compactors can perform compaction operations adapting to ground surface changes and can determine working width and number of units based on available power *(Tolon-Becerra A., Tourn M., Botta G.F., Lastra-Bravo X., 2011; Botta G.F., Tolon-Becerra A., Tourn M., Lastra-Bravo X., Rivero D., 2012)*. Other types include tubular compactors, toothed disc compactors, anti-spray compactors, spiral compactors, double-sided tooth-meshing compactors, straight-faced fan compactors, and chrysanthemum-type compactors, all with varying degrees of application. Despite extensive research on soil compaction machinery by domestic and international scholars, studies on compaction machinery specifically for rice seedling greenhouses remain insufficient. Existing machinery struggles to achieve ideal compaction effects while meeting the dimensional requirements of rice seedling greenhouses.

Therefore, there is a need to design an efficient compaction mechanism suitable for use within greenhouses to reduce manual labor and improve seedbed soil firmness, thereby promoting crop growth. Through the Recurdyn-EDEM coupling method and eccentric vibration theory, an eccentric block-shaft motion model is established and numerically simulated to provide a theoretical basis for the design and optimization of soil compaction machinery for rice seedling greenhouses.

MATERIALS AND METHODS

Agronomic requirement

According to the "Technical Specifications for Intelligent Soil Preparation Equipment Testing in Standardized Rice Seedling Greenhouse Seedbeds" formulated by the National Grassroots Agricultural Technology Extension System Reform and Construction Project of the Beidahuang Group, the agronomic requirement for standardized rice seedbeds is "firm on top, loose below". Measurements of the 0-0.45 m soil layer should yield soil firmness values as shown in Table 1.

Table 1

Reference Range for Soil Firmness After Leveling

Soil depth [m]	0~0.15	0.15~0.30	0.30~0.45
Soil solidity [kPa]	2600~2800	3000~3300	1800~2000

Referring to the provisions in "GB/T 5 668-2017", the post-tillage surface evenness is used as the performance evaluation indicator for seedbed leveling machines. The post-tillage surface evenness is measured perpendicular to the direction of machine advancement. A horizontal baseline is established above the highest point of the ground surface. At appropriate positions, a width equivalent to the working width of the prototype machine is divided into 10 equal parts. The distance from each division point to the ground surface is measured, and the average and standard deviation of these measurements are calculated. One point is measured for each pass, and the average of the standard deviations under working conditions represents the evenness. A post-tillage surface evenness of 0.05 m or less is considered satisfactory.

Based on these agronomic requirements, when designing a rice seedling greenhouse seedbed leveling machine, special attention must be paid to the design of the compaction device. On one hand, this device needs to effectively compact the surface soil to meet the required firmness standards. On the other hand, it must avoid over-compacting the lower soil layers to ensure the necessary looseness for root system growth, thereby meeting the evenness requirements specified in "GB/T 5 668-2017" *(Gang C., Wei L., Lin W., 2023).*

The whole machine structure and principle

The seedbed compaction device consists of a frame, gearbox, eccentric shaft mechanism, and counterweight box. The frame is composed of a body and a baseplate, with connection holes for the landing gear at the front end of the frame, and the frame bottom welded to the baseplate. The gearbox is a T6 spiral bevel gear reducer. The eccentric shaft mechanism comprises a main shaft, eccentric block, bearings, and bearing housings. The eccentric block is a solid iron block with a notch, allowing adjustment of its tightness against the main shaft by varying the depth of the adjusting screw. The counterweight box consists of compression springs and a weighted iron box. The power connection device is achieved through a fixed coupling, with power output connected to the tractor's output shaft via a universal joint. The speed is then increased through the gearbox and transmitted via V-belts to drive the eccentric shaft's rotation as shown in Figure 1.

The working process of the seedbed compaction device utilizes the rotation of the main shaft with its eccentric block to induce vibration in the entire machine, thereby causing continuous vibration of the counterweight box. As the tractor moves forward during operation, it pulls the machine, which to some extent contributes to leveling the ground.

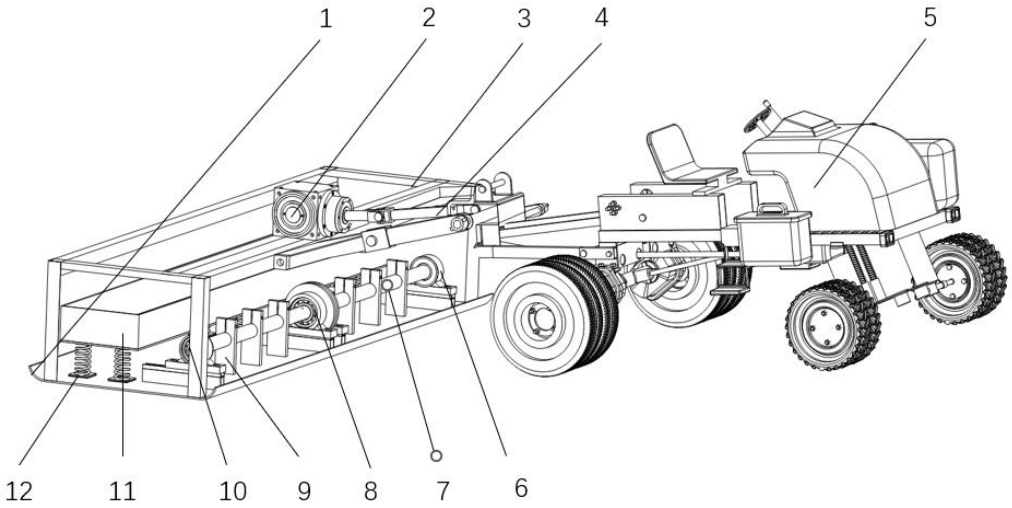

Fig. 1 –Overall Machine Structure

1. bottom plate; 2. transmission; 3. racks; 4. output shafts; 5. front; 6. bearing seats; 7. spindle; 8. belt wheels; 9. bearing; 10. bearings; 11. weight boxes; 12. main vocal spring

Motion equation

This paper employs an eccentric block structure. To facilitate manufacturing and reduce costs, a simpler block structure is used as shown in Figure 2. The excitation force generated by the eccentricity is:

$$F_{(t)} = m_1 e \omega^2 \quad (1)$$

where:

m_1 is the mass of the eccentric block, [kg]; e is the eccentricity, [m]; ω is the angular velocity of the eccentric block rotation, [rad/s].

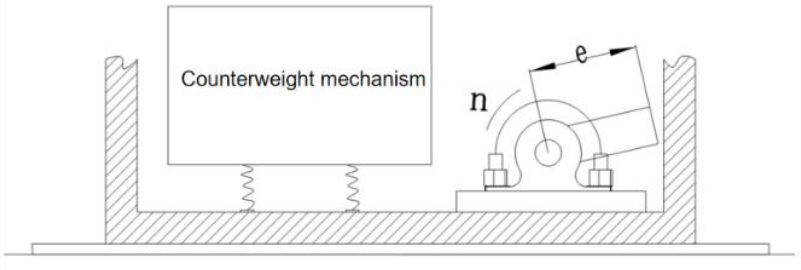

Fig. 2 –Simplified Motion Diagram of the Leveling Machine

The spring deformation is:

$$x = \frac{F_{(t)} - F_0}{k} \quad (2)$$

where:

F_0 is the restoring force of the spring [N]; k is the spring stiffness coefficient, [N/mm].

According to Newton's second law, the springs system motion equation is:

$$m_2 \frac{d^2x}{dt^2} + kx = m_1 e\omega^2 \quad (3)$$

where:

m_2 is the weight of the counterweight mechanism [kg];

Based on trigonometric identities, the amplitude can be derived as:

$$A = \frac{m_1 e\omega^2}{k - m_2\omega^2} \quad (4)$$

Based on agronomic requirements for a maximum soil firmness of 3300 kPa and design specifications allowing engine output speeds of 0 ~ 104.72 rad/s during operation, an excitation force of 4500 N is selected at 62.83 rad/s. This results in an eccentricity of 0.045 m, although typical eccentric mechanisms like vibrating screens generally use an eccentricity of 0.020 m *(Olumide O., Indresan G., Njema M.A., et al., 2021)*.

To meet the agronomic requirement of a maximum seedbed soil firmness of 3300 kPa, the leveling machine must exert a significant downward force to ensure effectiveness. This necessitates a greater excitation force to achieve the required working amplitude. However, increasing the excitation force also increases the load, leading to reduced service life, increased energy consumption, and compromised machine reliability and cost-effectiveness. Therefore, drawing inspiration from large vibrating screen mechanisms, main vibration springs are installed beneath the tamping box. This increases the amplification factor of the vibration system, allowing the vibration system to resonate with the excitation system, thereby reducing power output burden and increasing amplitude. This effectively addresses the lifespan issues of key components, saves manual labor, and improves work efficiency.

Based on the agronomic requirement for maximum soil firmness of 3300 kPa and design specifications, the natural frequency of the compaction mechanism components is observed to ensure that internal structures do not resonate near the working frequency. The main vibration springs are then designed to bring the overall system's working frequency close to the natural frequency of 10 Hz for the vibration mode moving vertically up and down. When the overall system resonates, deformation primarily occurs in the elastic elements, allowing the internal structure of the compaction mechanism to be approximated as a rigid body *(Thiago B.L., Classon B.S.V., 2021)*. This ensures internal structural stability and reliability while effectively reducing excitation force, extending the service life of shafts and bearings, and reducing the vibrating screen's energy consumption. Resonance occurs when the excitation frequency ω equals the system's natural frequency ω_0, where:

$$\omega = \omega_0 = \sqrt{\frac{k}{m_2}} \quad (5)$$

The equation of motion at this point becomes:

$$m_1 \frac{d^2x}{dt^2} + c\frac{dx}{dt} + kx = m_1 e\omega^2 - m_2 \quad (6)$$

where: c is the damping coefficient, [N·s/m].

Calculations show that the springs can withstand a maximum load of 5000 N. With a stiffness coefficient of 1400 N/mm, the system's natural frequency is 10 Hz. The maximum load on the springs is a combination of the excitation force and the weight of the counterweight box, so the maximum weight of the counterweight box is 500 N, approximately 51.02 kg. In the subsequent simulation, the weight of the counterweight box is tentatively set at 50 kg.

The relationship between frequency and amplitude

According to previous calculations, after adding springs, the system's natural frequency is around 10 Hz, matching the excitation frequency. Resonance occurs when the excitation frequency is approximately 10 Hz, significantly increasing the amplitude to meet design requirements (*Zhang C., 2020*). Using RecurDyn software to solely consider the leveling machine's motion state, the spring stiffness coefficient is set to 1400 N/mm. Displacement conditions are captured within 1-1.5 seconds of movement on the Ground at shaft rotation speeds of 52.36 rad/s (8 Hz), 62.83 rad/s (10 Hz), and 75.40 rad/s (12 Hz) to observe the overall machine vibration and further verify if it meets design requirements in Figure 3.

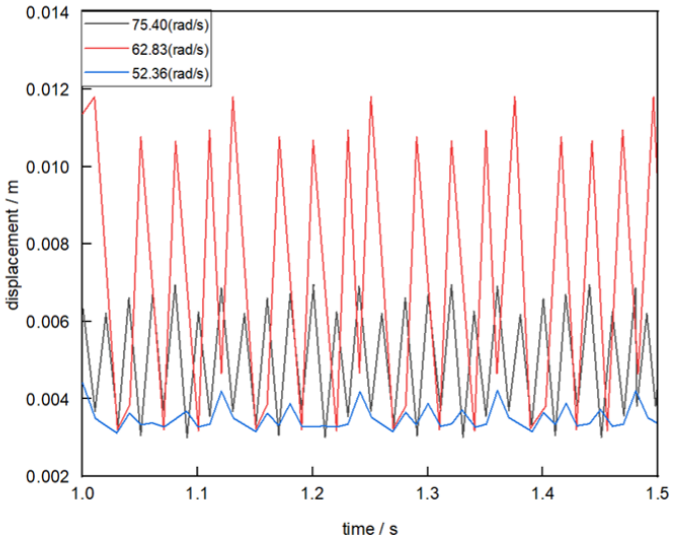

Fig. 3 –Relationship between excitation frequency and amplitude

The Z-axis displacement of the leveling machine at 52.36 rad/s (8 Hz), 62.83 rad/s (10 Hz), and 75.40 rad/s (12 Hz) is exported from RecurDyn. As the eccentric shaft speed (excitation frequency) increases, the overall machine amplitude shows a trend of first increasing and then decreasing *(Lamandé et al, 2011)*. The maximum amplitude shown in the figure is 0.01082 m, with a vibration frequency of 9.86 Hz, which is close to both the excitation frequency and the previously calculated natural frequency, aligning with the expected design plan.

Model establishment

A simplified three-dimensional structural model of the seedbed leveling machine was created using SolidWorks 2020 and saved as an .x_b file. This file was then imported into the RecurDyn multibody dynamics simulation software. The soil compaction process of the leveling machine was simulated using the EDEM-RecurDyn coupling method *(Ucgul M., Fielke J.M., Saunders C., 2014).* The main parameters of the constructed seedbed soil compaction simulation model are shown in Table 3.

Table 3

Main Parameters of the Soil Particle Model

Parameter name	Value
Soil particles density [kg/m^3]	2740
Soil particle shear modulus [Pa]	1.55e+08
Soil particle Poisson's ratio	0.29
Coefficient of restitution between soil particles	0.4
Static friction coefficient between soil particles	0.4
Dynamic friction coefficient between soil particles	0.11
Surface energy between soil particles [J/m^2]	0.159
Static friction coefficient between soil and leveling machine	0.5
Soil-Separate Rubbing coefficient between the leveling machines	0.48
Dynamic friction coefficient between soil and leveling machine	0.21

Comparison verification

To validate the significant effect of using an eccentric mechanism for soil compaction in the seedbed leveling machine, this study employed a comparative analysis method. The performance of traditional compaction devices (weight dragging), compaction mechanisms without springs, and compaction mechanisms with added springs were systematically evaluated.

First, a simplified model of the compaction mechanism was constructed in the multibody dynamics simulation software RecurDyn. For the traditional compaction device, the entire structure was set as a rigid body with an applied forward motion speed of 0.6 m/s to simulate actual operating conditions. Second, for the compaction mechanism without springs, the sand box and spring were set as a rigid body, with the eccentric block's shaft rotation speed set to 62.83 rad/s and a forward motion speed of 0.6 m/s, to study the effect of the eccentric mechanism on soil compaction performance. Finally, for the compaction mechanism with added springs, a spring system was introduced based on the above settings, with a stiffness coefficient set to 1400 N/mm. By setting the eccentric block's shaft rotation speed to 62.83 rad/s and maintaining a forward motion speed of 0.6 m/s, the contribution of the added spring system to soil compaction effectiveness could be comprehensively evaluated.

To obtain reliable experimental data, each mechanism underwent three repeated trials. By comparing and analyzing the changes in soil firmness under different operating conditions, the advantages of the seedbed leveling machine's eccentric mechanism in soil compaction could be objectively evaluated *(Lamande M., Greve M.H., Schjonning P., 2018)*.

The results of this study indicate that compared to traditional compaction devices and compaction mechanisms without springs, the compaction mechanism with added springs can significantly improve soil compaction effectiveness. This provides important evidence for optimizing the design of seedbed leveling machines.

Based on actual soil conditions, through the selection and parameter settings of the soil trough model, and utilizing features such as the contact model in EDEM software, the actual operation of the implement can be replicated. The reliability of the simulated test results can be restored. Since EDEM software cannot calculate complex motions such as eccentric vibrations and spring elastic support, RecurDyn software is used to add motion and import it into EDEM to simulate and explore the distribution patterns of soil firmness *(Elskamp F., Kruggel-Emden H., Hennig M., et al. 2015).* Figure 4 shows the distribution of contact forces between soil particles at different depths during the compaction process of the leveling machine on seedbed soil. In the figure, a higher concentration of red particles indicates greater soil firmness in that area *(Sun J., Chu H., Liu Q., 2022)*.

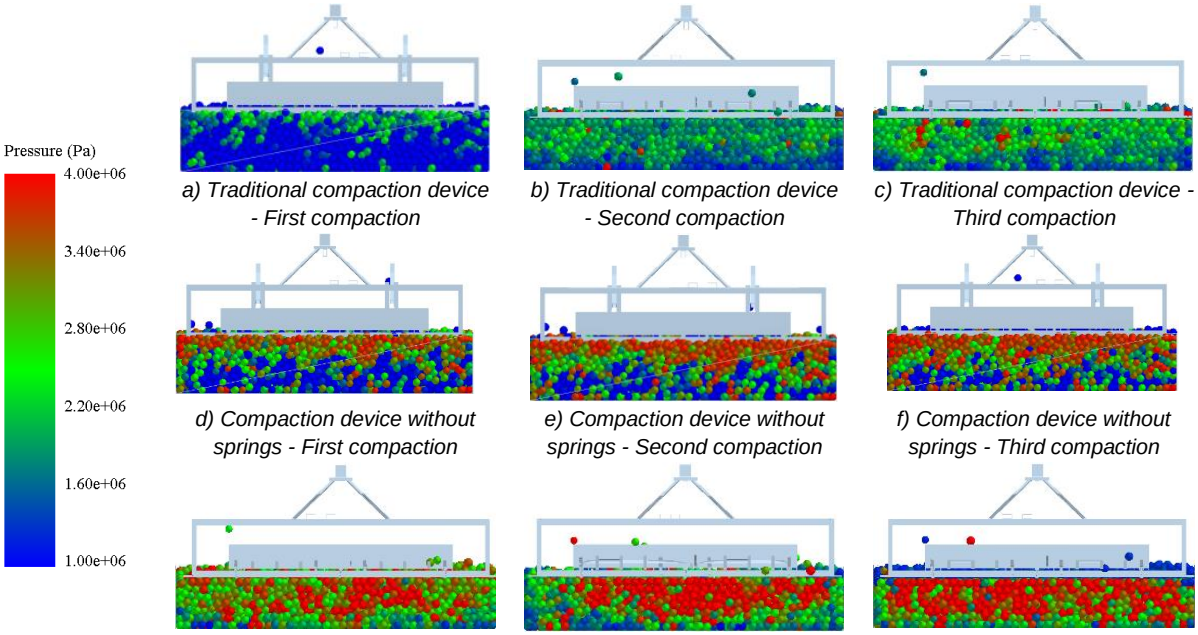

a) Traditional compaction device - First compaction
b) Traditional compaction device - Second compaction
c) Traditional compaction device - Third compaction
d) Compaction device without springs - First compaction
e) Compaction device without springs - Second compaction
f) Compaction device without springs - Third compaction
g) Compaction device with springs - First compaction
h) Compaction device with springs - Second compaction
i) Compaction device with springs - Third compaction

Fig. 4 – Comparative validation of different compaction devices

In summary, through the comparative analysis of the performance of different institutions in the soil consolidation of the soil, this study provides strong evidence, indicating that the application of eccentric institutions in the setting of the seedbed can significantly improve the effect of soil consolidation and meet the high standard requirements of modern agricultural production.

As shown in Figure 4c, the traditional compaction device cannot meet agronomic requirements. Data exported from the EDEM post-processing module after three compactions shows that the maximum firmness value in the 0-15 cm soil layer is 1820.2 kPa. In actual production, the mass of the compaction device is similar to that of the leveling machine, making the simulation results quite convincing.

Figure 4f indicates that the leveling machine without springs meets agronomic requirements in the 0 ~ 0.15 m soil layer after the third compaction. Although no springs are added, the eccentric mechanism can provide small-amplitude vibrations. The average firmness of five points in the 0.15 ~ 0.30 m soil layer is 2650.7 kPa, which does not meet the agronomic requirement range of 3000-3300 kPa. The smaller amplitude provides less downward force, and due to the internal friction characteristics of soil particles, energy cannot be transferred to deeper soil layers when the amplitude is small. Only by continuously increasing the shaft rotation speed can agronomic requirements be met.

As shown in Figure 4i, the firmness in the 0 ~ 0.15 m layer is 2770.4 kPa, 3124.1 kPa in the 0.15 ~ 0.30 m layer, and 1802.6 kPa in the 0.30 ~ 0.45 m layer. This meets the agronomic requirement of "firm on top, loose below" and aligns with practical needs, further validating the significant effect of the leveling machine compared to traditional compaction devices.

In conclusion, through systematic comparative analysis of different mechanisms' soil compaction performance, this study provides strong evidence that the application of eccentric mechanisms in seedbed leveling machines can significantly improve soil compaction effectiveness, meeting the high standards required in modern agricultural production.

Simulation test of seedling bed levelling machine

Single factor test

Single-factor experiments were conducted using machine forward speed, eccentric shaft rotation speed, and counterweight box mass as factors, with soil firmness and evenness as performance indicators. This was done to determine the influence patterns of each factor on the evaluation indicators of the leveling machine. When testing the motion parameters of the leveling machine's eccentric device, parameters were reset in Recurdyn and imported into EDEM for simulation, completing single-factor experiments of the leveling machine's motion parameters based on preliminary test results.

When the machine forward speed was in the range of 0.2 ~ 1.2 m/s, simulation revealed that the speed value should not be too high or too low. The front part of the compaction machine levels the surface soil of the seedbed, pushing the surface soil forward to "fill holes with pushed soil" as shown in Figure 5.

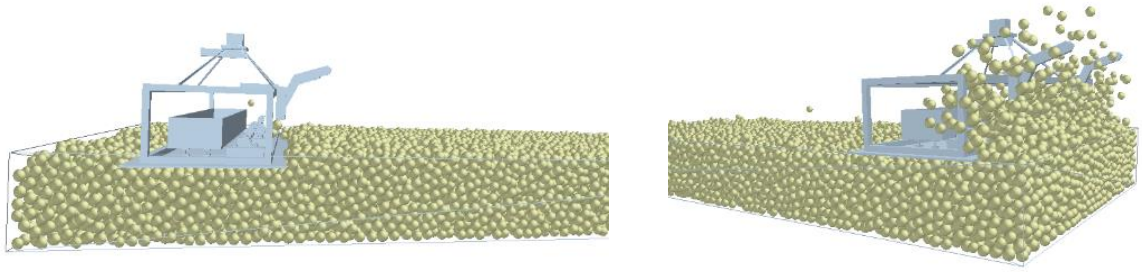

Fig. 5 – Effect of machine forward speed on seedbed

When the speed was in the range of 0.2 ~ 0.5, due to the low speed, too much soil accumulated at the front, causing the machine to stall in the field. When the speed was in the range of 0.9 ~ 1.2 m/s, the high speed caused severe scattering of soil particles during the pushing process.

When the machine forward speed was in the range of 0.5 ~ 0.9 m/s, soil firmness showed a gradual decreasing trend, while evenness did not change significantly. The test results are shown in Figure 6. This is because lower machine forward speeds result in higher compaction frequency per unit soil area, transferring more energy. As the machine forward speed increases, the compaction frequency per unit soil area decreases, leading to a gradual decrease in soil firmness in Figure 6. Therefore, a machine forward speed range of 0.5 ~ 0.9 m/s was selected for multi-factor experiments.

The eccentric shaft rotation speed is an important parameter of the leveling machine's motion, directly affecting the overall machine amplitude. The eccentric shaft drives the eccentric block, with faster rotation speeds resulting in higher excitation frequencies. Although the motion was simulated on a relatively ideal plane in previous sections, in reality, the interaction between the machine and soil also has some impact on the

motion. When the eccentric shaft rotation speed was in the range of 54.45 ~ 70.16 rad/s, soil firmness showed a trend of first increasing and then decreasing, while evenness showed a trend of first decreasing and then increasing, generally tending towards stability. When the eccentric shaft speed was below 54.45 rad/s, the amplitude clearly did not meet the design amplitude requirements and could not satisfy agronomic requirements after three compactions. Therefore, an eccentric shaft rotation speed range of 54.45 ~ 70.16 rad/s was selected in Figure 6.

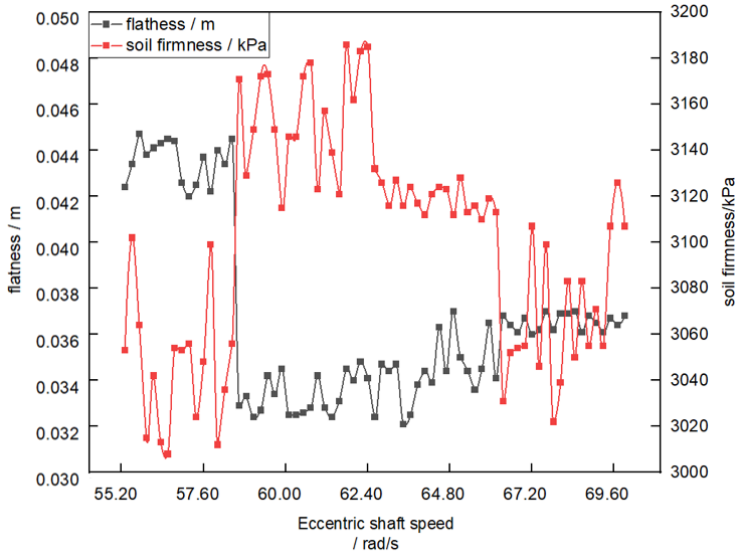

Fig. 6 – Effect of Eccentric Shaft Rotation Speed on Evaluation Indicators

The mass of the counterweight box provides static pressure for the compaction machinery, helping to maintain stable contact with the ground and transmitting pressure to the surface during compaction. The increased mass of the counterweight box adds inertia to the entire system, resulting in a more stable and controllable vibration response when the eccentric block generates excitation force. The mass of the counterweight box, together with the spring stiffness coefficient, determines the system's natural frequency. By changing the mass of the counterweight box, the system's natural frequency can be adjusted. During the compaction process, the counterweight box and spring system can store and release energy. When the eccentric block moves upward, the spring is compressed, increasing potential energy; when it moves downward, the spring releases energy, transferring it to the baseplate and ground, achieving the compaction function. When the counterweight box mass is less than 40 kg or greater than 50 kg, the main vibration spring compression does not meet design requirements and cannot achieve the designed amplitude. Therefore, the selected range for the counterweight box mass is 40 ~ 60 kg in Figure 7.

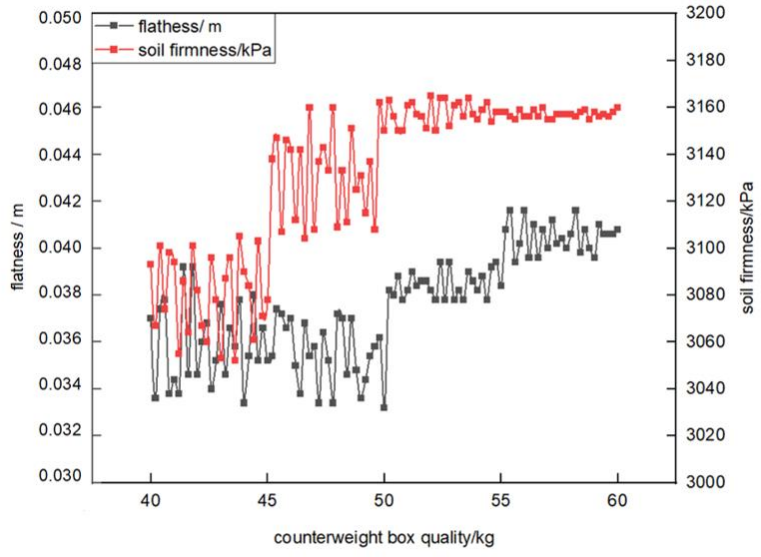

Fig. 7– Effect of Counterweight Box Mass on Evaluation Indicators

Parameter optimization experiment for compaction mechanism

Based on single-factor experiment results, the ranges for machine forward speed X_1, eccentric shaft rotation speed X_2, and counterweight box mass X_3 were determined. Referring to GB/T 5 668-2017, soil firmness at 15-30 cm depthY_1 and evennessY_2 were selected as performance evaluation indicators for the leveling machine. A three-factor, five-level quadratic orthogonal rotational central composite design was adopted. The experimental table was generated using Design-Expert software, with each group of experiments repeated 3 times. The coding of experimental factors is shown in Table 4.

Table 4

Factor horizontal coding table

Level	Coding Value	Forward speed X_1 [m/s]	Eccentric shaft speed X_2 [rad/s]	Counterweight box mass X_3 [kg]
Upper star arm (+1.682)	+1.682	1	70.16	70
Upper level(+1)	+1	0.9	67.02	60
Zero level(0)	0	0.7	62.83	50
Lower level(-1)	-1	0.5	58.61	40
Lower star arm (1.682)	-1.682	0.4	55.50	30

Table 5

Test data table

Serial number	Experimental factors			Test indicators	
	Forward speed X_1 [m/s]	Eccentric shaft speed X_2 [rad/s]	Counterweight box mass X_3 [kg]	Firmness [kPa]	Evenness [m]
1	-1	-1	1	3037.2	0.25
2	0	0	0	3165	0.37
3	0	0	0	3155.3	0.17
4	0	0	0	3131.7	0.02
5	0	0	0	3158.1	0.27
6	-1	1	1	3039.6	0.26
7	1	-1	-1	2963.5	0.02
8	0	0	0	3157	0.31
9	-1.68179	0	0	3025.6	0.22
10	1	1	-1	3022	0.05
11	0	-1.68179	0	2998.3	0.18
12	1.68179	0	0	3010.7	0.36
13	0	0	1.68179	3027.2	0.28
14	0	1.68179	0	3035.6	0.04
15	0	0	-1.68179	2988.2	0.01
16	0	0	0	3163.3	0.38
17	-1	-1	-1	3008.7	0.23
18	0	0	0	3163.6	0.02
19	-1	1	-1	3033.9	0.22
20	1	1	1	3036.1	0.04
21	0	0	0	3156.9	0.01
22	0	0	0	3160.2	0.32
23	1	-1	1	3027.3	0.35

After regression fitting using Design-Expert software, regression equations for the effects of various factors on soil firmness and evenness were obtained. Variance analysis and significance results analysis showed that all three regression variances were significant ($P<0.01$), while the lack of fit P-value was not significant, indicating that the fitting of each regression equation was relatively optimal. Regression equations for the coded values of each factor were established.

$$Y_1 = 3156.456 - 6.997X_1 + 11.54225X_2 + 13.011X_3 + 4.962X_1X_2 + 5.462X_1X_3 - 9.062X_2X_3 - 45.819X_1^2 - 46.243X_2^2 - 49.514X_3^2$$
$$Y_2 = 2.778 - 0.193X_1 - 0.407X_2 - 0.223X_3 + 0.187X_1X_2 - 0.387X_1X_3 + 0.312X_2X_3 \quad (7)$$

Analysis of test results

Figure 8a shows the effect of the interaction between eccentric shaft speed and forward speed on soil firmness when the counterweight box mass is 50 kg. The graph indicates that at a constant forward speed, as the eccentric shaft speed increases, soil firmness first increases and then decreases. When the eccentric shaft speed is constant, lower forward speeds result in higher firmness.

Figure 8b illustrates the effect of the interaction between counterweight box mass and forward speed on soil firmness when the eccentric shaft speed is 62.83 rad/s. The graph shows that at a constant forward speed, as the counterweight box mass increases, soil firmness first increases and then decreases. When the counterweight box mass is constant, lower forward speeds result in higher firmness.

Figure 8c depicts the effect of the interaction between counterweight box mass and eccentric shaft speed on soil firmness when the forward speed is 0.7 m/s. The graph reveals that as both counterweight box mass and eccentric shaft speed increase, soil firmness first increases and then decreases.

Figure 8d shows the effect of the interaction between eccentric shaft speed and forward speed on evenness when the counterweight box mass is 50 kg. The graph indicates that as both eccentric shaft speed and forward speed increase, evenness first rises and then falls. The eccentric shaft speed has a more significant impact on evenness.

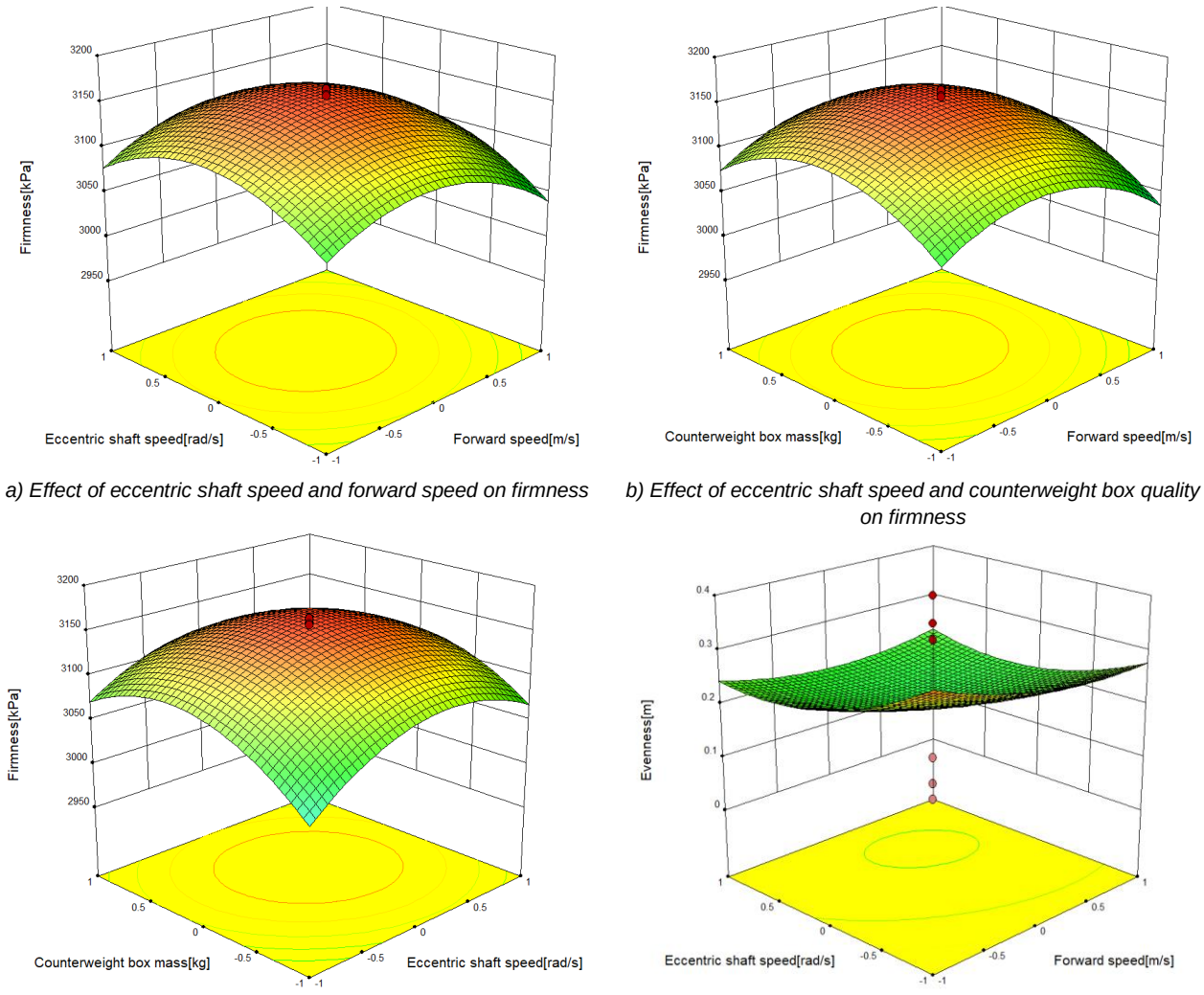

a) Effect of eccentric shaft speed and forward speed on firmness

b) Effect of eccentric shaft speed and counterweight box quality on firmness

c) Influence of forward speed and counterweight box mass on firmness

d) Influence of eccentric shaft rotation speed and advance speed on flatness

Fig. 8 – Response surface of each interaction factor to the evaluation indicators

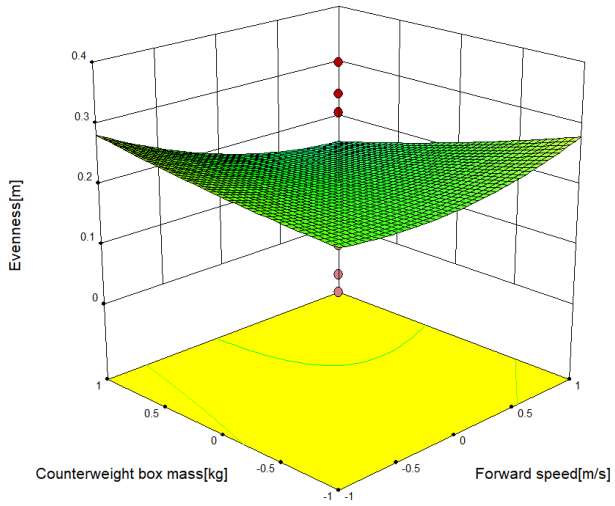

e) Effect of eccentric shaft speed and counterweight box quality on flatness

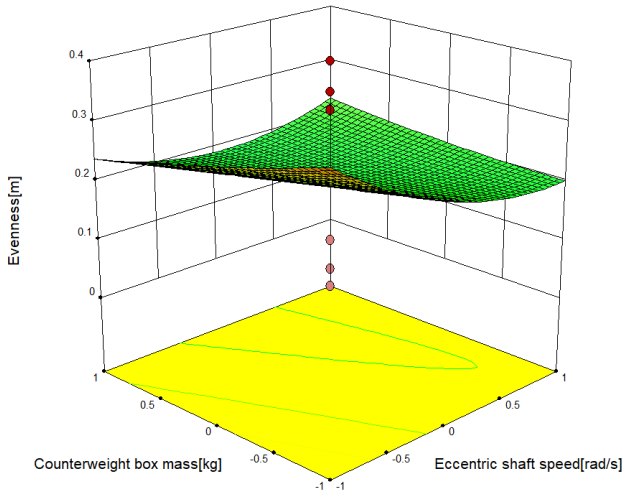

f) Effect of forward speed and counterweight box quality on flatness

Fig. 8 – Response surface of each interaction factor to the evaluation indicators

Figure 8e illustrates the effect of the interaction between eccentric shaft speed and counterweight box mass on evenness when the forward speed is 0.7 m/s. The graph shows that as both eccentric shaft speed and counterweight box mass increase, evenness first increases and then decreases.

Figure 8f depicts the effect of the interaction between forward speed and counterweight box mass on evenness when the eccentric shaft speed is 62.83 rad/s. The graph reveals that as both forward speed and counterweight box mass increase, evenness first increases and then decreases. The eccentric shaft speed has a more significant impact on evenness.

Optimization and verification

Through simulation experiments with different parameter settings for the leveling machine's working device, the interactive effects of various experimental factors on soil firmness and evenness were obtained. Design-Expert software was used to optimize the data and establish a mathematical model expression as follows:

$$\begin{cases} \begin{matrix} max\, Y_1 \\ min\, Y_2 \end{matrix} \\ s.t \begin{cases} 0.5\ m/s \ \leq X_1 \leq 0.9\ m/s \\ 58.61\ rad/s \leq X_2 \leq 67.02\ rad/s \\ 40\ kg \leq X_3 \leq 60\ kg \\ 3000\ kPa \leq Y_1(X_1, X_2, X_3) \leq 3300\ kPa \\ 0.01\ m \leq Y_2(X_1, X_2, X_3) \leq 0.04\ m \end{cases} \end{cases} \quad (8)$$

Using Design-Expert software for optimization, when the machine forward speed is 0.708 m/s, eccentric shaft rotation speed is 63.23 rad/s, and counterweight box mass is 50.99 kg, the soil firmness is 3156.554 kPa, and evenness is 0.025 m.

FIELD TEST

Test materials and equipment

The experiment was conducted in a greenhouse at Heilongjiang Bayi Agricultural University in Figure 9. Greenhouse No. 1 was selected as the experimental field, with dimensions of 60m × 12m and a moisture content of 15.1%. A Jinhe 2ZG-8KZ high-speed rice transplanter was used as the power source for the seedbed leveling machine. Operating parameters were controlled to be consistent with the simulation values for the rice seedling greenhouse experiment.

A DSA320 level and a TYY-2 soil hardness tester were used to measure soil elevation and firmness, respectively. Five points were sampled and averaged to meet the agronomic requirements of "GB/T 5 668-2017".

Fig. 9 – Field test

Test process and analysis

After the leveling experiment, multiple measurement points were evenly distributed in the test area for soil data collection. A level and soil hardness tester were used to measure seedbed soil elevation and firmness.

Following land leveling operations, the operational effect was evaluated by analyzing and comparing the relative errors of data obtained before and after the operation. Relevant indicators such as evenness and soil firmness were introduced to assess the operational effect.

The evaluation standard for leveling operations is the evenness after operation, which is assessed using the standard deviation of relative field surface elevations. Evenness is calculated according to equation (9):

$$S_i = \sqrt{\sum_{i=1}^{n} (h_i - \bar{h})^2 / n - 1} \quad (9)$$

where: S_i is the evenness, [m]; h_i is the relative elevation of the i-th sampling point in the field; $\bar{h}$ is the expected relative elevation for the field, [m]; generally refers to the average relative surface elevation of all measurement points within the field, i.e., the average design elevation, [m]; n is the number of all sampling points within the field.

A diagonal method was used to determine firmness sampling points in the selected area. Eleven points were evenly spaced along each diagonal, as shown in Figure 10. A TYY-2 soil hardness tester was used to measure seedbed soil firmness at 0.015 ~ 0.030 m depth. Firmness was measured and compared before and after the operation.

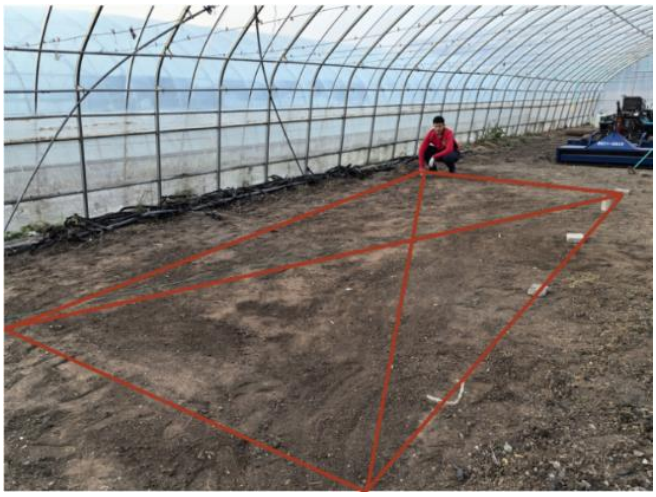

Fig. 10 – Diagonal point taking

After practical verification, the intelligent soil preparation machine for standardized rice seedling greenhouse seedbeds achieved the agronomic requirement of "firm on top, loose below". After the experiment, the evenness was 0.034 m, and the firmness at 0.015 ~ 0.030 m depth was 3102.5 kPa, meeting the agronomic requirements of "GB/T 5 668-2017".

RESULTS

Test results and analysis

The data recorded by the elevation meter was exported and processed using Origin 2021 software to obtain the seedbed evenness, as shown in Figure 11.

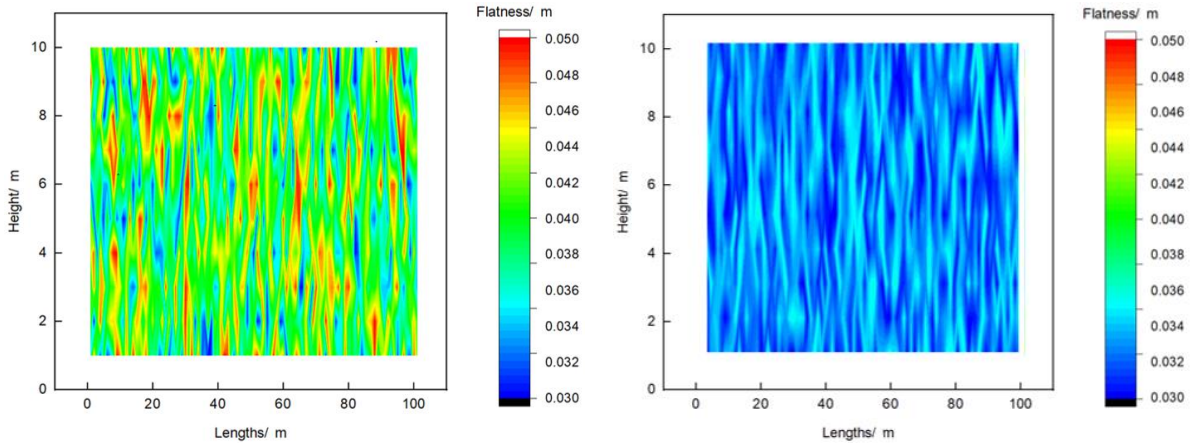

a) pre-test *b) post-test*

Fig. 11 – Ground evenness before and after experiment

Software calculations revealed that before the experiment, the red and yellow areas occupied 43.75% and 25.1% of the total area respectively, while the blue and green areas accounted for 31.15%. After three operations, the red and yellow highlighted areas decreased to 1.2% and 12.2%, while the blue and green areas increased to 86.6%. Therefore, the rice seedling greenhouse seedbed leveling machine had a significant effect on seedbed soil evenness.

During the rice soil preparation period in the experimental greenhouse at Heilongjiang Bayi Agricultural University, data on actual operational efficiency and seedbed firmness were collected for three seedbed leveling methods: traditional compaction device, compaction device without springs, and compaction device with springs. The results are shown in Figure 12.

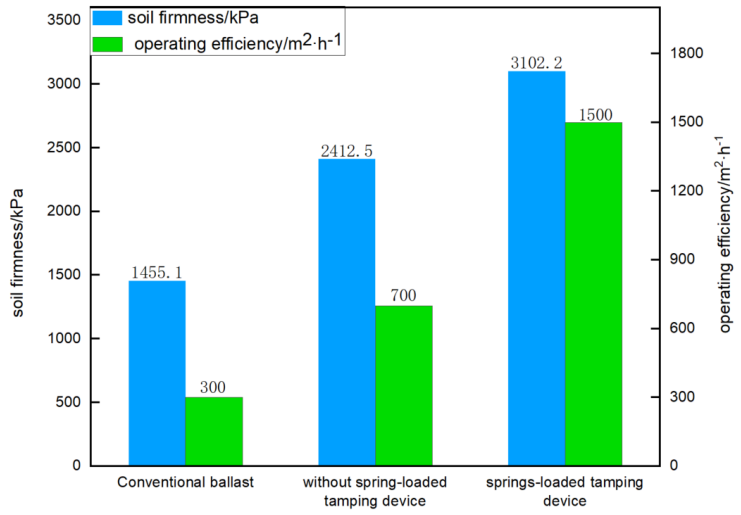

Fig. 12 – Comparison of leveling operation effects

Using the traditional compaction device for seedbed leveling operations could only level 300 m²/h of seedbed, with poor leveling effects that required repeated operations. The application of the compaction device with springs for seedbed leveling operations could level approximately 1550 m²/h of seedbed. The experimental results show that the leveling operation efficiency increased by about 400% compared to the traditional compaction device and by about 114.29% compared to the compaction device without springs.

The relative errors between the optimal simulation parameters and actual operation results are shown in Table 5 below:

Table 5

Optimization and test results

Project	Soil firmness [kPa]	Flatness [m]
Optimization results	3156.554	0.0257
Actual results	3102.5	0.026
Relative error /%	1.75	2.3

The optimal parameter combination: machine forward speed of 0.708 m/s, eccentric shaft rotation speed of 63.23 rad/s, and counterweight box mass of 50.99 kg resulted in soil firmness of 3156.554 kPa and evenness of 0.02573 cm. The experimental results were within 5% relative error of the simulation optimization results, indicating that the seedbed soil firmness and evenness meet agronomic requirements and have practical application value.

CONCLUSIONS

To optimize the performance of the compaction device for rice seedling greenhouses and improve seedbed soil firmness and evenness, this paper analyzed and studied the main parameters affecting compaction effectiveness through theoretical analysis, simulation modeling and experimental validation. The factors influencing seedbed soil firmness were analyzed: a motion model of the compaction device was established, and the relationships between eccentric shaft rotation speed, eccentric block mass, spring stiffness coefficient, counterweight mechanism mass and amplitude were derived.

A soil compaction mechanism suitable for rice seedling greenhouse seedbeds was designed. RecurDyn software was used to simulate the compaction process. Results showed that when the vibration frequency was 9.86 Hz, the amplitude reached a maximum of 0.0108 m, which aligned with the expected design plan.

RecurDyn-EDEM coupling was used to simulate the compaction process, resulting in optimal combination parameters of 0.708 m/s for machine forward speed, 603.84 r/min for eccentric shaft rotation speed, and 50.99 kg for counterweight box mass. Field trials showed that the relative error between actual results and optimized results was less than 5%.

ACKNOWLEDGEMENT

This project is the special project of Central Government guiding local Science and Technology development (ZY20B05); National Grassroots Agricultural Technology Extension Project (NJ202105);

REFERENCES

[1] Botta G.F., Tolon-Becerra A., Tourn M., Lastra-Bravo X., Rivero D. (2012). Motion resistance and soil compaction in relation to tractor design and different soil conditions. *Soil & Tillage Research*, Vol.120, pp.92-98. Argentina.

[2] Elskamp F., Kruggel-Emden H., Hennig M., et al. (2015). Benchmarking of process models for continuous screening based on discrete element simulations. *Minerals Engineering*, Vol. 83, pp. 78-96. Germany.

[3] Gang C., Wei L., Lin W. (2023). Design and test of automatic leveling system for rice seedling shed seedbed precision leveler (水稻秧棚苗床精平机自动调平系统设计与试验). *Journal of Agricultural Engineering*, Vol. 39, pp. 9-17, Heilongjiang /China.

[4] Jia L., Jiang Y., Sun J., et al. (2021). Simulation and test of disc rotary roller of disc elastic tooth combined paddy field grader based on EDEM (基于 EDEM 的圆盘弹齿组合式水田平地机圆盘转辊仿真与试验). *Journal of Jiangxi Agricultural University*, Vol.06, pp.202-210, China.

[5] Lamandé M., Greve M.H., Schjonning P. (2018). Risk assessment of soil compaction in Europe-Rubber tracks or wheels on machinery. *Catena*, Vol.167, pp.353-362. Denmark.

[6] Lamandé M., Schjonning P., (2011). Effect of soil water content. *Soil and Tillage Research*, 114, 78-85.

[7] Luo H., Meng Y., Li X. (2019). Three-dimensional model study of ridge no-tillage seeder (垄作免耕播种机三维模型研究). *Rural Economy and Science and Technology*, Vol.30, pp.68-70, China.

[8] Olumide O., Indresan G., Njema M.A., et al. (2021). Development of a mechanistic model of granular flow on vibrating screens. *Minerals Engineering*,Vol.163 , pp. 67-71. Cape Town /South Africa.

[9] Sun J., Chu H., Liu Q. (2022). Research on soil compaction stress of hill track tractor contour operation on slopes (山地履带拖拉机坡地等高线作业土壤压实应力研究). *Journal of Agricultural Machinery*, Vol.53, pp.30-42, Shanxi /China.

[10] Thiago B.L., Classon B.S.V. (2021). Analysis of the dynamic forces acting on a vibrating screen and its support structure using a scale mode. *Measurement*, Vol.176, pp. 109-116. Brazil.

[11] Tolon-Becerra A., Tourn M., Botta G.F., Lastra-Bravo X. (2011). Effects of different tillage regimes on soil compaction, maize (*Zea mays L*.) seedling emergence and yields in the eastern Argentinean Pampas region. *Soil & Tillage Research*, Vol.117, pp.184-190. Spain.

[12] Ucgul M., Fielke J.M., Saunders C. (2014). Three-dimensional discrete element modelling of tillage: determination of a suitable contact model and parameters for a cohesionless soil. *Biosystems Engineering*, Vol.121, pp. 105-117. Australia.

[13] Zhang C. (2020). High stiffness elastic support design of inertia vibrating screen (惯性振动筛的高刚度弹性支撑设计). *Journal of Hubei University of Technology*, Vol. 35, pp. 22-27, Hubei /China.

[14] Zhang Y., Huang H., Ren L., (2013). Research on soil cutting test and drag reduction mechanism of bionic bucket teeth of excavator (挖掘机仿生斗齿土壤切削试验与减阻机理研究). *Journal of Agricultural Machinery*, Vol.44, pp.264-267. China.